Enhanced range-doppler algorithm for SAR image formation

Enhanced range-doppler algorithm for SAR image formation

M Sakr[1], A S Amein[2], F M Ahmed[1], G M Amer[3], A Youssef[1]

[1] Electrical Engineering, Military Technical College, Cairo, Egypt.
[2] Faculty of Information and Computer Science, October 6 University, Giza, Egypt.
[3] Electrical Engineering, Faculty of Engineering, MUST University, Giza, Egypt

E-mail: sakrmtc@gmail.com

Abstract. A Synthetic Aperture Radar (SAR) system is a powerful source of information due to its capability to operate day and night and in all weather conditions. It is essential for military and civilian purposes. Pulse-focusing is employed by the SAR system for achieving both long-range detection and fine-range resolution. The Range-Doppler Algorithm (RDA) is the most popular pulse-focusing technique for creating images from coherent SAR data. Pulse compression techniques for SAR signal processing targets seek to improve map resolution, lower peak power, and increase the Signal-to-Noise Ratio (SNR) of the detected object. This paper demonstrates an enhanced RDA algorithm that uses a modified pulse compression technique based on mismatched filter optimization where Quadratic Constrained Quadratic Program (QCQP) is used. The performance evaluation of the proposed method is performed using visual assessment and the standard image quality metrics peak-side-lobe-ratio (PSLR), impulse-response-width (IRW), and integrated-side-lobe-ratio (ISLR). Simulated and real SAR raw data are used for performance evaluation. The experimental results demonstrate the proposed method's robustness, efficiency, and reliability in providing a higher-quality SAR image than the traditional RDA algorithm.

Keywords: Synthetic Aperture Radar (SAR), Pulse Compression, Range-Doppler Algorithm, Convex Optimization, Side Lobe Level.

1. Introduction

Synthetic Aperture Radar (SAR) is a type of active microwave remote-sensing technology utilized to obtain an image of a scene [1]. It has the capability of operating all day or night and under any weather conditions [2]. There are many algorithms that are used to improve the SAR image formation process and image quality. According to the required application, the most suitable algorithm is applied [3]. The Range-Doppler Algorithm (RDA) is the most commonly used SAR imaging algorithm since it is uncomplicated, makes motion compensation simple, and provides a flexible way to balance accuracy and calculation time [4]. RDA employs pulse compression techniques to enhance the detection range and range resolution of long pulses. To do this, the transmitted pulse is modulated, and the received signal and the transmitted pulse are correlated [2]. In high-power radar systems, linear frequency modulation (LFM), frequently called the chirp signal, is widely used. The LFM signal achieves a greater level of resolution by combining a matching filter with the pulse compression method [4]. The SAR point target can be defined using specific parameters such as impulse-response-width (IRW), peak-side-lobe-ratio (PSLR),

and integrated-side-lobe-ratio (ISLR). The IRW is the measurement of the main lobe width at 3 dB below its peak value. The PSLR is the ratio of the main lobe's peak amplitude to the side lobe that is most obvious, while the ISLR is the total side lobe power divided by the main lobe power ratio [4]. The measurements for both parameters are expressed on a logarithmic scale.

In the case of applying a single target to a matched filter, the output has a PSLR value of around -13 dB as shown in figure 1(a). On the other hand, applying multiple targets having different scattering values can cause problems by interfering with the Signal-to-Noise Ratio (SNR), reducing the resolution of the imaging system, and increasing the complexity of the analysis. These issues can lead to inaccurate measurements, degraded image quality, and a higher degree of uncertainty in the data [5]. As a result, the powerful scatters' sidelobes conceal the weak targets causing degradation of the image quality and an impact on potential post-processing steps like target identification and recognition as shown in figure 1(b).

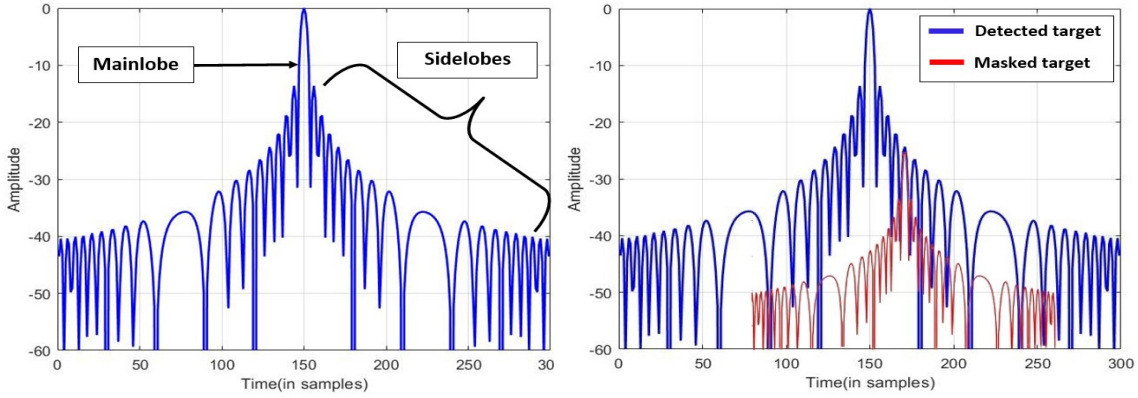

(a) **(b)**

Figure 1. (a) A matched filter's main and side lobes for a single target. (b)The side lobes of the detected target include a concealed target.

The high PSLR is a challenge in SAR imaging. An approach that is widely used to address this high PSLR issue is using window functions, such as Taylor, Hamming, Kaiser, and Hann, Blackman windows at the reception side with different trade-offs [5]. Window functions may, however, widen the main lobe and reduce the SNR when applied to matched filter at the receiving side, which negatively impacts SAR image resolution [6]. Therefore, from the perspective of optimization, it makes sense to construct a mismatched filter. One of the most powerful tools to solve this problem is Quadratic Constrained Quadratic Program (QCQP) [7]. QCQP is a convex optimization technique, including interior point methods, that resolves the PSLR problem [8].

This paper presents a modified version of RDA that utilizes an optimized mismatched filter to lower side lobe levels without the need for additional weighting or windowing functions [6]. The method is based on addressing the PSLR optimization problem as an identical QCQP [9]. The paper is structured as follows: section (2) gives a summary of conventional RDA, section (3) outlines the methodology for the proposed algorithm, section (4) demonstrates the use of the proposed algorithm in SAR point target simulation and real raw data, and compares it to conventional RDA algorithms using window functions through visual and quantitative assessments in MATLAB simulation. Finally, section (5) presents the conclusion.

2. Range-Doppler Algorithm

RDA was presented in 1978 as an algorithm that efficiently utilizes Fast Fourier Transforms (FFT) to condense the azimuth and range direction of the unfocused raw SAR data [6]. It is the most widely utilized SAR processing technique [10], in addition, it consistently and effectively accounts for range-varying features including range cell migration, azimuth frequency modulation rate, and doppler centroid [4], as seen in figure 2.

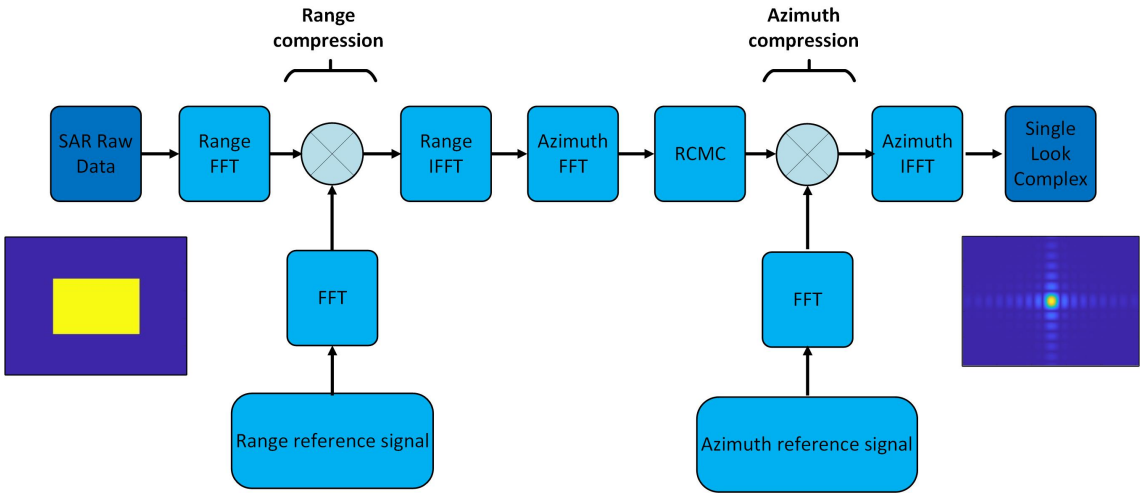

Figure 2. Basic RDA block diagram.

The process of range-Doppler processing in radar imaging is designed to improve the resolution and accuracy of the images produced [2]. It begins with a fast convolution that compresses the range of the data, followed by the multiplication of the raw data in the frequency domain with a range reference function [10]. This results in calculating the range FFT, multiplication with a matched filter, and applying the range inverse FFT [6]. An azimuth FFT is employed to transform the data into the Range-Doppler domain.

Range migration, which is caused by fluctuations in the range data due to platform movement, is corrected through a process called range cell migration correction (RCMC). This step effectively straightens the path of the data [2]. Subsequently, azimuth compression is applied along every parallel azimuth line, resulting in a single cell where all the energy in the path is focused [4]. Before performing the final inverse FFT, the data is passed through a matched filter to further improve its accuracy. Finally, the data is converted back to the time domain using an azimuth inverse FFT, resulting in a highly accurate and compressed complex image [10].

The topic of SAR pulse compression has been the subject of several research studies. In [5], traditional tapering windows with LFM signal are altered and utilized to suppress side lobe in compressed pulses, resulting in a compressed radar pulse with a maximum SLL of around -43 dB. The expansion of the main lobe and reduction in processing gain are the prices for this. In [4], utilizing stretch and correlation processing techniques, a highly compressed pulse with a maximum SLL of about -23.8 dB is produced. In [11], range compression in SAR image focusing is solved utilizing a variety of adaptive processing algorithms, and both realistic and ideal evaluations are conducted. In [12], a technique for compressing radar pulses is connected to the creation of effective non LFM waveforms. This method results in a pulse radar that is compressed with SLL of around -40 dB.

3. Methodology

This section presents a proposed approach for improving imaging performance in SAR systems. The approach involves incorporating an optimization technique based on the QCQP algorithm in the PSLR sense into the RDA. The steps outlined in this section are as follows:

3.1 Optimization model for mismatched filter

The target area is acquired by the SAR system's signal, which is followed by the processing of the echoes to provide visual information [13]. Take into account a signal vector $\mathbf{s}$ with N samples: $\mathbf{s} = [s_1, s_2, \ldots, s_N]^T$. After a filter $\mathbf{P}_{M\times 1}$ of length $M = N + 2l \geq N$ with $l \geq 0$ has processed the output Y at the receiving side, it may be represented as:

$$Y_{(M+N-1)\times 1} = \Lambda_M(\mathbf{s})\ \mathbf{P}_{M\times 1}. \tag{1}$$

The signal vector $\mathbf{s}$ forms the matrix $\Lambda_M(\mathbf{s})$, a correlation matrix of size $(M+N-1)\times M$, as shown below:

$$\mathbf{\Lambda}_M(\mathbf{s}) = \begin{bmatrix} s_N & 0 & \cdots & \cdots & \cdots & \cdots & 0 \\ \vdots & s_N & \ddots & & & & \vdots \\ s_2 & \vdots & \ddots & 0 & & & \vdots \\ s_1 & s_2 & \cdots & s_N & 0 & \cdots & 0 \\ 0 & s_1 & \ddots & \vdots & s_N & \ddots & \vdots \\ \vdots & \ddots & \ddots & s_2 & \vdots & \ddots & 0 \\ 0 & \cdots & 0 & s_1 & s_2 & \cdots & s_N \\ \vdots & & & 0 & s_1 & \ddots & \vdots \\ \vdots & & & & \ddots & \ddots & s_2 \\ 0 & \cdots & \cdots & \cdots & \cdots & 0 & s_1 \end{bmatrix}_{(M+N-1)\times M} \tag{2}$$

The matched filter scenario, whose output may be represented as $Y_{\mathrm{MF}} = \mathbf{\Lambda}_N(\mathbf{s}) \cdot \mathbf{s}^*$, is well known to increase the energy at the peak response as $p = \mathbf{s}^*$, which implies $M = N$. In this case, the vector $\mathbf{s}^* = (s_1^*, s_2^*, \cdots, s_N^*)^\top$ represents the conjugate operator, denoted as $(\cdot)^*$, which makes it the best choice for single-target problems. However, it could provide side lobes that are quite high. Therefore, it may not be appropriate for multitarget problems when the side lobe level is crucial.

Instead of using a window function, we optimized the reference signal at the receiving side to produce higher image performance. The objective is to find a sequence $\mathbf{p}$, a mismatched filter coefficient, that reduces the filter's PSLR output, hence:

$$\begin{aligned} &\min_{\mathbf{p}} \|\mathbf{Fy}\|_\infty \\ &\text{s.t. } \mathbf{s}^H\mathbf{p} = \mathbf{s}^H\mathbf{s}. \end{aligned} \tag{3}$$

Minimax optimization is required to resolve this issue where $\|\mathbf{X}\|_\infty = \max_i |x_i|$ represents the infinity norm. $\mathbf{F}$ represents a diagonal one's matrix, with the exception of the indexes that indicate the location of the main lobe [13]. The LFM signal's main lobe width is represented by the number of zeros in the diagonal's center (in points), from which we can detect the signal's side lobe. In such a situation, it is simple to get rid of any constraints controlling the main lobe's peak level that may otherwise alter the main lobe's shape. The first constraint here in equation (3) is to prevent the null solution.

A convex QCQP approach is taken to resolve the PSLR issue, which is amenable to efficient solutions by numerical methods [9]. Any feasible solution that is discovered

is guaranteed to be a PSLR global optimal issue due to the convexity of the proposed method. Additionally, the formulation's adaptable structure allows for the insertion of any additional constraints that might be relevant to the situation. The requirement that all side lobe points must be fewer than a certain value is the second restriction, which is subsequently minimized. It was observed that the equation (3) in the minimax optimization may be rewritten as follows:

$$\begin{aligned} &\min_{\mathbf{p},r} r \\ &\text{s.t. } \mathbf{s}^H\mathbf{p} = \mathbf{s}^H\mathbf{s} \\ &(\lambda_{N+l+j}(\mathbf{s})\mathbf{p})^H \times (\lambda_{N+l+j}(\mathbf{s})\mathbf{p}) \leq r, |j| > N_{\mathrm{ML}}. \end{aligned} \tag{4}$$

The minimax optimization issue demonstrates that it is quadratically constrained, where $\mathbf{r}$ is the magnitude of PSLL that has to be optimized, and $(N + l + j)$th is the row of the matrix $\Lambda_M(\mathbf{s})$ that represents $\lambda_{N+l+j}(\mathbf{s})$. The quantity of samples present in the right main lobe is referred to as N_{ML}.

Adopting a mismatched filter might further reduce PSL at the price of loss-in-processing gain (LPG) [7], even if, a matched filter is necessary for the receiver in the presence of additive white gaussian noise [8]. This LPG may be described as the difference between the ideal SNR at the output of the mismatched filter $\mathrm{SNR}_{\mathrm{mismatched}}$ and the SNR of the matched filter $\mathrm{SNR}_{\mathrm{matched}}$. As a result, the sentence may be rewritten as follows:

$$\begin{aligned} \text{SNR Loss } &= 10\log_{10}\left(\frac{\mathrm{SNR}_{\mathrm{mismatched}}}{\mathrm{SNR}_{\mathrm{matched}}}\right) \\ &= 10\log_{10}\left(\frac{\left|\mathbf{p}^H\mathbf{s}\right|^2}{\left(\mathbf{p}^H\mathbf{p}\right)\left(\mathbf{s}^H\mathbf{s}\right)}\right) \leq 0. \end{aligned} \tag{5}$$

Adding the equal energy constraint($\mathbf{s}^H\mathbf{p} = \mathbf{s}^H\mathbf{s}$), the formula is derived as follows:

$$\text{LPG Loss } = 10\log_{10}\left(\frac{\mathbf{s}^H\mathbf{s}}{\mathbf{p}^H\mathbf{p}}\right). \tag{6}$$

As a result, the third constraint in this collection, the loss-in-processing gain constraint indicated by β, is similarly convex since the constraint is a positive semi-definite quadratic and is identical to $\mathbf{p}^H\mathbf{p} \leq \alpha \times \mathbf{s}^H\mathbf{s}$ where $\alpha = 10^{-\beta/10} \geq 1$ and $(\beta \leq 0)$. Consequently, the issue with optimization will be

$$\begin{aligned} &\min_{\mathbf{p},r} r \\ &\text{s.t. } \mathbf{s}^H\mathbf{p} = \mathbf{s}^H\mathbf{s} \\ &\mathbf{p}^H\mathbf{p} \leq \alpha \times \mathbf{s}^H\mathbf{s} \\ &(\lambda_{N+l+j}(\mathbf{s})\mathbf{p})^H \times (\lambda_{N+l+j}(\mathbf{s})\mathbf{p}) \leq r, |j| > N_{\mathrm{ML}}. \end{aligned} \tag{7}$$

Including set value constraints for the main lobe of the peak level might be one feasible solution. Generally, any samples of the filter output can have some fixed value limitations added. We may use $\mathbf{a} = (a_{-N_{\mathrm{ML}},}, a_{-N_{\mathrm{ML}}+1} \cdots, a_{-1}, a_0, a_1, \cdots, a_{N_{\mathrm{ML}}-1}, a_{N_{\mathrm{ML}}})^\top$ as the main lobe constraint. With the addition of the fourth main lobe constraint, the

optimization problem becomes:

$$\begin{aligned}
&\min_{\mathbf{p},r} r \\
&\text{s.t. } \mathbf{s}^H\mathbf{p} = \mathbf{s}^H\mathbf{s} \\
&\mathbf{p}^H\mathbf{p} \le \alpha \times \mathbf{s}^H\mathbf{s} \\
&(\lambda_{N+l+j}(\mathbf{s})\mathbf{p})^H \times (\lambda_{N+l+j}(\mathbf{s})\mathbf{p}) \le r, |j| > N_{\mathrm{ML}} \\
&(\lambda_{N+l+j}(\mathbf{s})\mathbf{p})^H \times (\lambda_{N+l+j}(\mathbf{s})\mathbf{p}) \le a_j, |j| \le N_{\mathrm{ML}}.
\end{aligned} \tag{8}$$

The nearest side lobe level, represented by (d), can be added as a fifth constraint. The value of (d) will be changeable in the PSLR optimization, providing insight into the distinct form of the side lobe. With the inclusion of the fifth restriction, the optimization problem will take the form:

$$\begin{aligned}
&\min_{\mathbf{p},r} r \\
&\text{s.t. } \mathbf{s}^H\mathbf{p} = \mathbf{s}^H\mathbf{s} \\
&\mathbf{p}^H\mathbf{p} \le \alpha \times \mathbf{s}^H\mathbf{s} \\
&(\lambda_{N+l+j}(\mathbf{s})\mathbf{p})^H \times (\lambda_{N+l+j}(\mathbf{s})\mathbf{p}) \le r, |j| > N_{\mathrm{nSL}} \\
&(\lambda_{N+l+j}(\mathbf{s})\mathbf{p})^H \times (\lambda_{N+l+j}(\mathbf{s})\mathbf{p}) \le d, N_{ML} \le |j| \le N_{\mathrm{nSL}} \\
&(\lambda_{N+l+j}(\mathbf{s})\mathbf{p})^H \times (\lambda_{N+l+j}(\mathbf{s})\mathbf{p}) \le a_j, |j| < N_{\mathrm{ML}}.
\end{aligned} \tag{9}$$

The Simulation Framework uses a specialized filter that was created and implemented in MATLAB, utilizing the CVX toolbox [8]. This toolbox allows for disciplined convex programming within MATLAB software. The filter utilizes the SDPT3 program to effectively solve convex quadratic problems with specified linear and quadratic constraints, making it a powerful tool for solving QCQP issues [9]. Consequently, the QCQP may be summed up as follows:

Algorithm 1: QCQP for mismatched filter design

Input : LFM signal $\mathbf{s}$
Main lobe width in points N_{ML}
loss-in-processing gain β
Ideal matched filter output Y_{matched}

Output: Mismatched filter coefficient $\mathbf{p}$

Step 1: Initialization

Step 2: Minimize PSLR and formulate convex optimization problem via QCQP based on side lobe and main lobe positions

s.t. $\mathbf{s}^H\mathbf{p} = \mathbf{s}^H\mathbf{s}$

$\mathbf{p}^H\mathbf{p} \le \alpha \times \mathbf{s}^H\mathbf{s}$

for *each,* $j \in N_{\mathrm{ML}} + N_{\mathrm{SL}}$ **do**

$(\lambda_{N+l+j}(\mathbf{s})\mathbf{p})^H \times (\lambda_{N+l+j}(\mathbf{s})\mathbf{p})$

end

Step 3: Add constraints for

- peak side level
- Side lobe magnitude
- Main lobe width
- Loss-in-processing gain
- level of the near side lobe

Step 4: Use CVX toolbox to obtain the mismatched filter coefficient, $\mathbf{p}$

3.2 Proposed RDA block diagram

The modified RDA, which utilizes the optimized mismatched filter in the range direction, is illustrated in figure 3. The process starts by optimizing the range reference LFM signal, which serves as the input data set for the standard RDA's range compression step, by applying the optimal technique described earlier in this section. In order to obtain the coefficient of the optimized mismatched filter and use it for the range compression step in the modified RDA, the reference signal is subjected to a convex optimization problem formulated using QCQP. This optimization is done under the constraints of peak side lobe level, main lobe width, side lobe magnitude, loss-in-processing gain, and the level of the near side lobe.

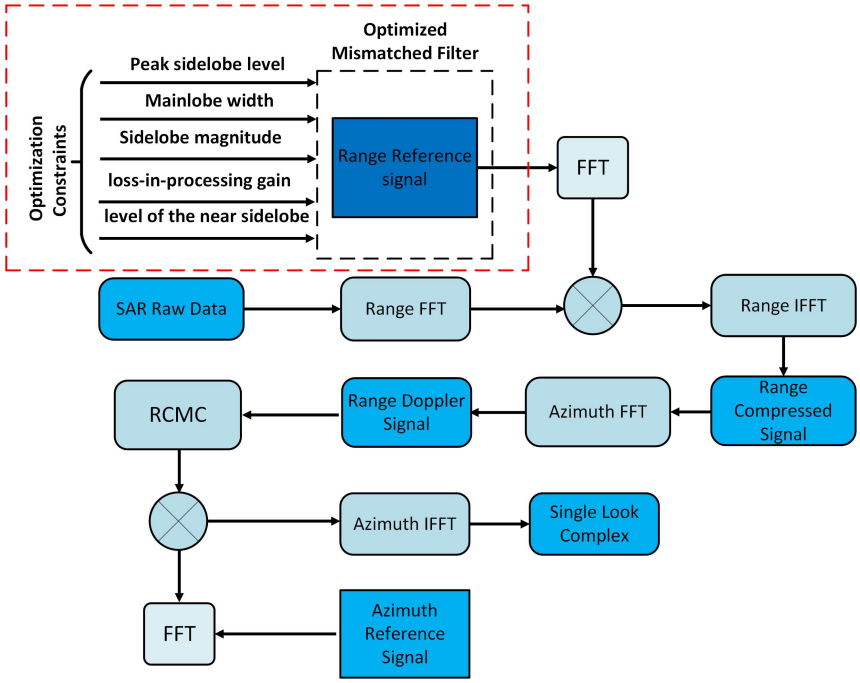

Figure 3. Proposed RDA block diagram.

The proposed algorithm begins by obtaining the mismatched filter coefficient $\mathbf{p}$ and using it to compress the range direction of the raw, unfocused SAR data. This is done by correlating the filter with the raw data. Once the range compression is completed, the remaining stages of the proposed algorithm are executed to generate the focused image, similar to the conventional RDA approach outlined in Section (2). The modified algorithm, as depicted in the block diagram, improves imaging performance and can handle various scenarios such as those requiring PSLR or SNR loss. It achieves this by suppressing side lobe levels without widening the main lobe width as the modified RDA utilizes the window function does. This approach effectively addresses the issue of strong scatter that could otherwise obscure weak targets in the range direction.

4. Experimental results and Performance evaluation

The performance of the proposed technique is assessed using different data sets to investigate the effectiveness of the proposed RDA based on the QCQP approach. The provided data sets contain SAR simulated point target data with sensor parameters illustrated in Table (1). and a real image from a European Remote Sensing satellite (ERS) in stripmap mode with ground sampling distance (along-track $\leq$ 30 m, cross-track $\leq$ 26.3 m).

Table 1. ERS SAR simulator parameters.

parameter	value	parameter	value
Carrier frequency (f_0)	5.3 GHZ	No. of range samples(N_{rg})	2048
(PRF)	1679.902 HZ	FM Rate Range Chirp (K_{r})	418.98 GHZ
Slant range (R_0)	852358.15 meter	Range sampling frequancy (f_{s})	18.962 GHZ
Chirp duration (T_{p})	37.12 μ sec	Wavelength (λ)	0.05656 m
Platform velocity(V)	7098.0194 m/s	No. of azimuth samples(N_{az})	2048

4.1 Results of the optimization model

Firstly, to show the effectiveness of the optimization approach indicated in section (3), an LFM signal with the parameters from Table 1, is fed into the optimization model. The convex optimization based on (QCQP) is used to get the coefficient of the optimized mismatched filter, using the toolbox CVX. Then applying the Kaiser window with the parameter ($\bar{B} = \mathbf{2.5}$) to the LFM signal. The Kaiser window is compared with the optimized mismatched filter output to determine the effectiveness of this approach. Figure 4 compares the improved model's output with the Kaiser window's output.

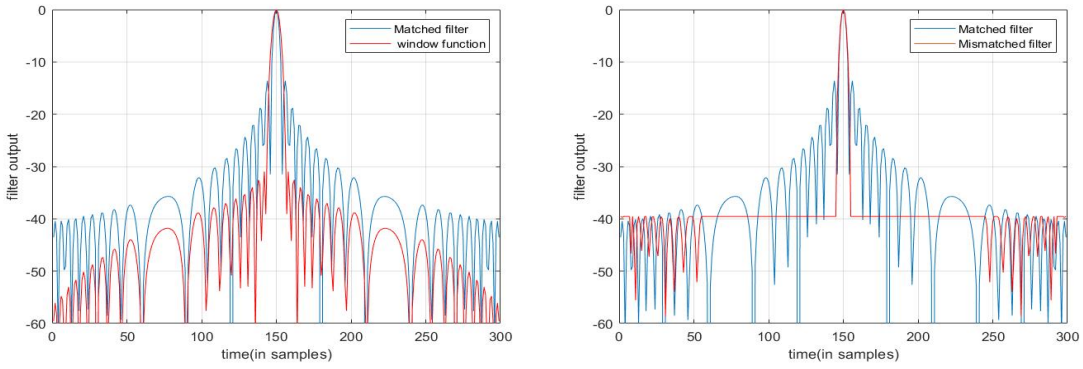

(a) The output of the Kaiser window. **(b)** The output of optimized mismatched filter.

Figure 4. (a) The output of the Kaiser window; (b) The output of the optimized mismatched filter.

As shown in figure 4(a), adding a Kaiser window with the parameter ($\bar{B} = \mathbf{2.5}$) to the output of a matched filter of LFM signal with side lobe level (PSLR $= -13.6186$ dB), results in a trade-off between narrowing the main lobe width and decreasing side lobe level to (PSLR $= -30.9723$ dB). However, as shown in figure 4(b), applying the optimized mismatched filter decreases the side lobe level to (PSLR $= -39.5752$ dB) without expanding the width of the main lobe. This demonstrates the advantages of the proposed method over the window function method.

4.2 Proposed image formation results

The proposed Image formation model performance is examined using simulated and real SAR data, then the results are compared to traditional RDA using the Kaiser window. The qualitative analysis will be as follows:

4.2.1 Results of simulated SAR point target. Using simulated raw data of a complex SAR signal for a point target located at a specific distance as an input data set,

a comparison of focused image output is performed for conventional RDA, RDA using Kaiser window, and proposed RDA using an optimized mismatched filter, shown in figure (5).

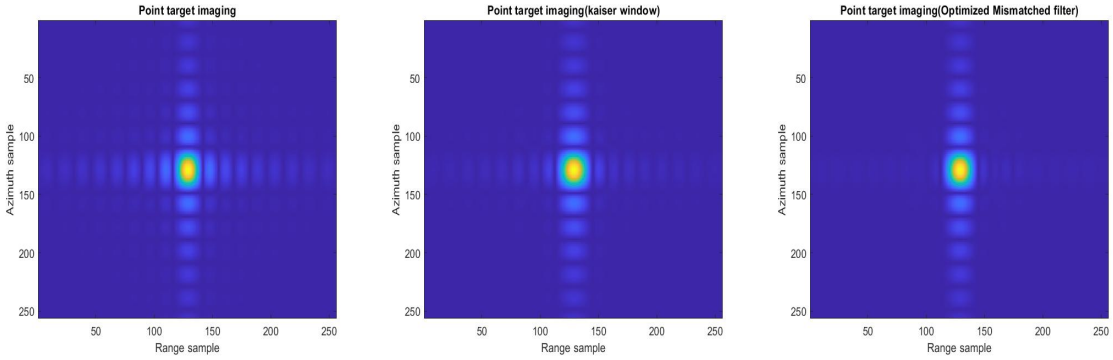

(a) Conventional RDA. **(b)** kaiser window. **(c)** Optimized mismatched filter.

Figure 5. (a) The output of the traditional RDA, (b) The output of the Kaiser window, (c) The output of the optimized mismatched filter.

As seen in figure (5), The output of the processed image using the point target model of conventional RDA is shown in Figure 5(a). The powerful scatters may obscure the weak targets in their side lobes since this model has a high side lobe level in the range direction. RDA utilizing the Kaiser window with parameter ($\bar{B} = \mathbf{2.5}$) is seen in figure 5(b), which suppresses the side lobe level but at the cost of the main lobe width and may have the same issue as the traditional RDA. The modified RDA in figure 5(c), utilizes an optimized mismatched filter to lower the side lobe level without sacrificing the main lobe width as the RDA with a window function, which has the advantage of preventing the weak targets from being hidden in the strong scatter's side lobes.

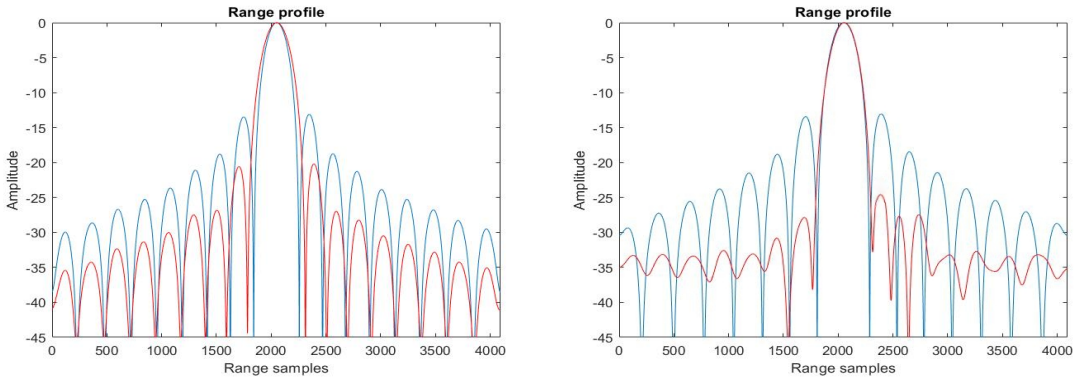

(a) The output of the Kaiser window. **(b)** The output of optimized mismatched filter.

Figure 6. (a) The output of the Kaiser window, (b) The output of the optimized mismatched filter.

Figure (6) displays the range profile for the RDA using the Kaiser window and the modified RDA with the optimized mismatched filter of the output of pulse compression in the range direction. Figure 6(a) shows the kaiser window output, which results in the reduction of (PSLR) to (-20.1898 dB) at the expense of the main lobe width. Figure 6(b). shows the optimized mismatched filter output, which decreased the side lobe level to (-25.2804 dB) in the range direction without widening the main lobe.

4.2.2 Results of real SAR data. The visual assessment is performed using the ERS dataset applied to the traditional RDA, RDA with Kaiser window, and the modified RDA, with a set of parameters obtained from the Table (1). In order to assess the performance of the proposed method, an area of interest (AOI) is selected, so that it contains a corner reflector that represents a strong target response, as shown in figure 7.

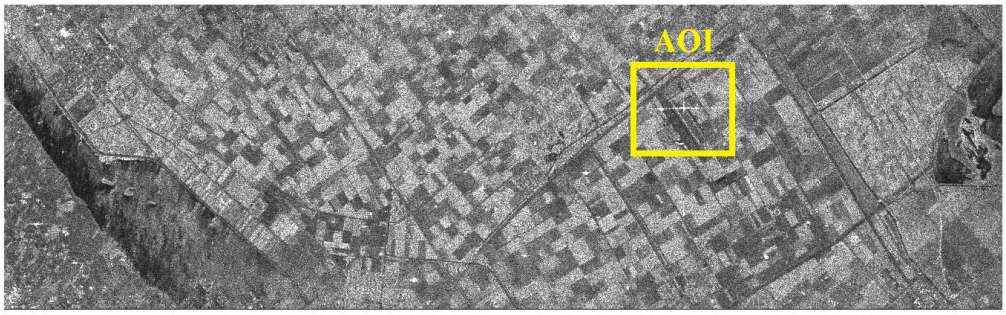

Figure 7. Focused image of ERS satellite produced by the Range Doppler Algorithm (RDA).

The highlighted square outlined in figure 7, referred to as the area-of-interest (AOI), will be the center of attention for a detailed analysis of the results obtained from three different image enhancement algorithms. This examination will be performed by zooming in on the designated area and comparing the improvements made by each algorithm, as illustrated in figure 8.

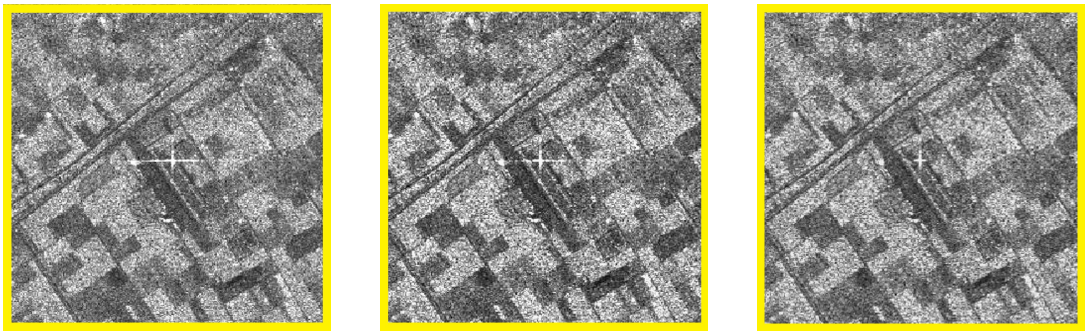

(a) Conventional RDA. **(b)** kaiser window. **(c)** Optimized mismatched filter.

Figure 8. (a) The output of the coventional RDA,(b) The output of the Kaiser window, and (c) The output of the optimized mismatched filter.

The output of a traditional RDA has a high scatter sidelobe, as shown in figure 8(a), which can affect weak targets in the range direction. The use of a Kaiser window in RDA, as depicted in figure 8(b), reduces the side lobe but scatter in the range direction may still be a problem. An optimized mismatched filter applied in the proposed RDA, as shown in figure 8(c), effectively reduces the side lobe of strong scatter and does not obscure weak targets in the range direction.

4.3 Performance Evaluation

The standard SAR image metrics, such as IRW, PSLR, and ISLR are the main quantitative parameters computed to test the SAR image quality. In the quantitative assessment for points, it is possible to assess these image quality parameters by modeling the Impulse

Response Function (IRF) from the point target response in SAR data and they are determined as [4]:

$$PSLR = 10 \log \frac{I_s}{I_m} \tag{10}$$

where I_s is the sidelobe peak intensity and I_m is the mainlobe peak intensity.

$$\text{ISLR} = 10 \log \frac{\int_{-\infty}^{a} |g(\tau)|^2 d\tau + \int_{b}^{\infty} |g(\tau)|^2 d\tau}{\int_{a}^{b} |g(\tau)|^2 d\tau} \tag{11}$$

where the mainlobe range is represented by (a, b), and $g(\tau)$ represents the function of the impulse response in the range or azimuth direction.

The proposed technique for mismatched filter design is evaluated through a numerical simulation, with the results presented in Tables (2) and (3). These tables compare the image quality formation results in the range direction for the proposed method, as well as the traditional RDA method and RDA with a window function, using the metrics IRW, PSLR, and ISLR.

Table 2. SAR point target simulation result.

Type	PSLR	ISLR	IRW
Conventional RDA	-13.1109 dB	-10.3473 dB	3.6012 m
Kaiser window	-20.1898 dB	-18.3809 dB	4.1936 m
Proposed RDA	-25.2804 dB	-24.0449 dB	3.7265 m

Table 3. SAR point target of ERS real data result.

Type	PSLR	ISLR	IRW
Conventional RDA	-13.1974 dB	-10.0583 dB	8.7144 m
Kaiser window	-20.2921 dB	-18.2676 dB	10.137 m
Proposed RDA	-26.0077 dB	-24.1454 dB	9.0184 m

The results shown in Tables (2) and (3) suggest that using an optimized mismatched filter in the RDA can improve the performance of the algorithm in terms of standard image metrics such as IRW, PSLR, and ISLR. The simulation results using the traditional RDA, RDA using a window function, and RDA using an optimized mismatched filter, show that the RDA using an optimized mismatched filter performs better than the other two methods in terms of suppressing side lobes while maintaining a narrow impulse response width.

The ERS real data results also support this conclusion, showing that the RDA model based on an optimized mismatched filter not only suppresses the side lobe level better than the modified RDA using the window function but also does not increase the main lobe width. This outcome indicates that the use of an optimized mismatched filter in RDA can effectively suppress the side lobes of strong scatters and maintain a high resolution, resulting in better image quality.

5. Conclusion

In this paper, SAR data compression using the proposed RDA has been presented, analyzed, and examined where the proposed approach is based on a mathematical model. The proposed approach utilizes an optimized mismatched filter based on QCQP and employs convex optimization, which is the primary distinction between the proposed and traditional algorithms. IRW, PSLR, and ISLR are used as quantitative metrics for the performance evaluation of the proposed approach. The results demonstrate that the proposed RDA method outperforms the standard RDA in terms of side lobe suppression and finer resolution in the case of using both the simulations and real SAR data. In addition, the experimental results indicate that the proposed method has robustness, reliability, and efficiency for providing a higher-quality SAR image compared to the traditional RDA algorithm.

References

[1] Eltanany A S, Amein A S and Elwan M S 2021 A modified corner detector for sar images registration *International Journal of Engineering Research in Africa* vol **53** (Trans Tech Publ) pp 123–156
[2] Cumming I G and Wong F H 2005 Digital processing of synthetic aperture radar data *Artech House* vol **1** (Boston) pp 108–110
[3] Fouad M A, Azouz A, Mashaly A A and Abdalla A E 2021 SAR image formation enhancement using effective velocity estimation method *International Conference on Aerospace Sciences and Aviation Technology* vol **19** (The Military Technical College) pp 1–9
[4] Ashry M M, Mashaly A S and Sheta B I 2022 Improved SAR range doppler algorithm based on the stretch processing architecture *2022 International Telecommunications Conference (ITC-Egypt)* vol **1** (IEEE) pp 1–6
[5] Galushko V 2020 On application of taper windows for sidelobe suppression in lfm pulse compression *2020 IEEE Ukrainian Microwave Week (UkrMW)* (IEEE) pp 995–1001
[6] Azouz A, Eldemiry A and Gaafar A 2018 New SAR algorithm for sidelobe reduction in range direction *The International Conference on Electrical Engineering* vol **11** (Military Technical College) pp 1–19
[7] Jin L, Wang J, Zhong Y and Wang D 2022 Optimal mismatched filter design by combining convex optimization with circular algorithm *IEEE Access* vol **1** pp 1–10
[8] Chatzitheodoridi M E, Taylor A and Rabaste O 2020 A mismatched filter for integrated sidelobe level minimization over a continuous doppler shift interval *2020 IEEE Radar Conference (RadarConf20)* vol **1** pp 1–6
[9] Boyd S, Boyd S P and Vandenberghe L 2004 Convex optimization *Cambridge University Press*
[10] Cruz H, Véstias M, Monteiro J, Neto H and Duarte R P 2022 A review of synthetic-aperture radar image formation algorithms and implementations: A computational perspective *Remote Sensing* vol **14** (MDPI) p 1258
[11] Dominguez E M, Magnard C, Frioud M, Small D and Meier E 2017 Adaptive pulse compression for range focusing in sar imagery *IEEE Transactions on Geoscience and Remote Sensing* vol **55** pp 2262–2275
[12] Vizitiu I C 2014 Some aspects of sidelobe reduction in pulse compression radars using nlfm signal processing *Progress In Electromagnetics Research C* vol **47** (EMW Publishing) pp 119–129
[13] Rabaste O and Savy L 2015 Mismatched filter optimization for radar applications using quadratically constrained quadratic programs *IEEE Transactions on Aerospace and Electronic Systems* vol **51** (IEEE) pp 3107–3122